PROCEEDINGS OF SCIENCE

Improved Calibration Methods and Reconstruction of the Underground Muon Detector of the Pierre Auger Observatory

Joaquín de Jesús [a,b,*] **for the Pierre Auger Collaboration**[c]

[a] *Instituto de Tecnología y Detección en Astropartículas (CNEA, CONICET, UNSAM), Buenos Aires, Argentina*

[b] *Karlsruhe Institute of Technolgy (KIT), Institute for Astroparticle Physics, Karlsruhe, Germany*

[c] *Observatorio Pierre Auger, Av. San Martín Norte 304, 5613 Malargüe, Argentina*

Full author list: https://www.auger.org/archive/authors_2024_11.html

E-mail: spokespersons@auger.org

As part of the upgrade of the Pierre Auger Observatory, known as AugerPrime, the Underground Muon Detector is being deployed in the low-energy extension of the Surface Detector. It comprises an array of 30 m^2 plastic scintillator muon counters, buried 2.3 meters underground near the water-Cherenkov detectors, allowing for direct measurement of the muonic component of air showers in the energy range of $10^{16.5}$ – 10^{19} eV. To achieve an extended dynamic range, the detector operates in two modes: the binary mode, which is optimized for low muon densities, and the ADC mode, designed for high muon densities. In this contribution, we present the latest improvements to the calibration procedure of the ADC mode and to the data reconstruction of the binary mode. We assess their performance with simulations.

The 7th International Symposium On Ultra High Energy Cosmic Rays
(UHECR2024)
17 – 21 November, 2024
Malargüe, Mendoza, Argentina

*Speaker

PoS(UHECR2024)077

1. Introduction

The Pierre Auger Observatory, the largest facility dedicated to studying ultra-high-energy cosmic rays (UHECRs), employs a hybrid detection technique for extensive air showers (EAS), combining a Surface Detector (SD) [1] and a Fluorescence Detector (FD) [2]. The SD, an array of 1660 water-Cherenkov detectors (WCDs) spaced 1500 m (SD-1500) apart in a triangular grid spanning 3000 km^2, measures the footprint of EAS particles on the ground. The FD, consisting of four sites equipped with fluorescence telescopes, observes the longitudinal development of the shower during moonless nights with good weather, enabling a quasi-calorimetric measurement of the shower energy.

Two nested, denser arrays of WCDs are deployed within a smaller area of the SD to extend the sensitivity of the Observatory to lower energies. The SD-750, with a 750 m spacing between the WCDs, covers an area of 23 km^2 and allows the detection of EAS with energies greater than $10^{17.3}$ eV. The SD-433, which has a spacing of 433 m, spans 1.9 km^2 and pushes the energy threshold down to $10^{16.5}$ eV. To enhance its sensitivity to primary mass, the Observatory recently underwent an upgrade known as AugerPrime [3], which included several improvements, such as the installation of scintillator and radio detectors on top of the WCDs, the replacement of the WCD electronics, and the deployment of the Underground Muon Detector (UMD).

2. Underground Muon Detector

The Underground Muon Detector (UMD) is being deployed in the SD-750 and SD-433 arrays. It consists of an array of plastic scintillator muon counters buried 2.3 m underground near a WCD. The soil above the detector absorbs the electromagnetic component of air showers and imposes an energy cut of ∼1 GeV for vertical muons. Each UMD station comprises three modules, made of 10 m^2 of plastic scintillator. A module is segmented into 64 strips, each 400 cm long, 4 cm wide, and 1 cm thick, with embedded wavelength-shifting optical fibers coupled to an array of 64 silicon photomultipliers (SiPMs). The UMD operates in slave mode with the WCD, relying on the latter to provide the trigger for data acquisition.

In order to increase the dynamic range of the UMD, two complementary modes of operation are implemented in the modules: the binary mode and the analog-to-digital converter (ADC) mode. The binary mode, designed for sampling low muon densities, relies on detector segmentation and processes each of the 64 SiPM signals independently. The output of each SiPM is processed by a dedicated channel, producing a binary trace of 2048 samples. In each sample, a "1" or "0" is recorded if the signal of the SiPM — after some electronic processing — was above or below a discriminator threshold, respectively. Muon signals in each bar are identified as a sequence of four or more consecutive "1"s, which we refer to as a *muon pattern* [4]. The number of bars with at least one muon pattern in their trace, k, serves as the basis for reconstructing the lateral distribution function (LDF) of muons in this mode. Details of this reconstruction are provided in Section 3.

On the other hand, the ADC mode, designed for high muon densities, treats the module as a whole independent of detector segmentation. In this mode, the 64 SiPM signals are summed and subsequently amplified with high- and low-gain amplifiers. The amplified signals are digitized with two ADCs at a sampling time of 6.25 ns, producing two waveforms of 1024 samples. The number

of muons is then obtained by dividing the charge of these signals by the mean charge of a single vertical muon $q_{1\mu}$. Therefore, $q_{1\mu}$ is the main parameter necessary for the ADC reconstruction. In Section 4, we present an improved method to determine $q_{1\mu}$ that accounts for the additional charge generated by knock-on electrons.

3. Reconstruction with the binary mode

3.1 Previous reconstruction procedure

The previous reconstruction method was based on the one proposed in Ref. [5] and was adopted to analyze the first data from the engineering array of the UMD [6]. The first step involved estimating the number of muons, $\hat{N}_\mu$, in each detector. This estimation was obtained by dividing the trace of each module into n_w time windows. In each window j, the number of bars with a muon pattern starting in that window, k_j, was determined and used to estimate the number of muons. The total number of muons in a detector was then obtained by summing over all time windows. A final zenith- and azimuth-dependent correction, derived from full detector simulations, was applied to account for overcounting caused by corner-clipping muons — inclined muons generating patterns in adjacent bars.

The likelihood of a detector was assumed to follow a Poisson distribution. Therefore, the estimated number of muons was introduced into a Poisson term

$$L_{\text{Poisson}}(\vec{p}) = \frac{e^{-\mu(\vec{p})}\mu(\vec{p})^{\hat{N}\mu}}{\hat{N}\mu!}, \tag{1}$$

where the expected number of muons is $\mu = \rho(r|\vec{p})A\cos\theta$, with $\rho(r|\vec{p})$ representing the muon density predicted by the LDF model (with parameters $\vec{p}$, which are to be estimated) evaluated at the detector position r, A is the area of the detector, and θ is the zenith angle of the shower. The geometry of the shower, from where r and θ are determined, is obtained independently by the SD. The event likelihood was constructed as the product of the likelihoods of each detector, and its negative logarithm was minimized to obtain the best-fit parameters $\vec{p}$ of the LDF. Saturated (modules having the 64 channels with a muon pattern in a time window) and non-triggered detectors (UMD modules paired to untriggered WCDs) were also considered for the LDF fit, see Ref. [6] for details.

3.2 Latest improvements in the reconstruction

Currently, several modifications have been implemented in the reconstruction chain of the binary mode of the UMD. Firstly, the use of time windows in the muon estimator has been discarded. As demonstrated in Ref. [7], the optimal performance of the estimator is achieved when no time windows are applied. Instead of using k_j, the current procedure is based on k, the total number of bars with at least one muon pattern during the event. It is worth noting that the use of k — rather than the k_js — as the foundational element of the reconstruction was first proposed in Ref. [9].

Secondly, the correction for overcounting due to corner-clipping muons, which was previously addressed solely through simulations, is now determined using the single-muon corner-clipping

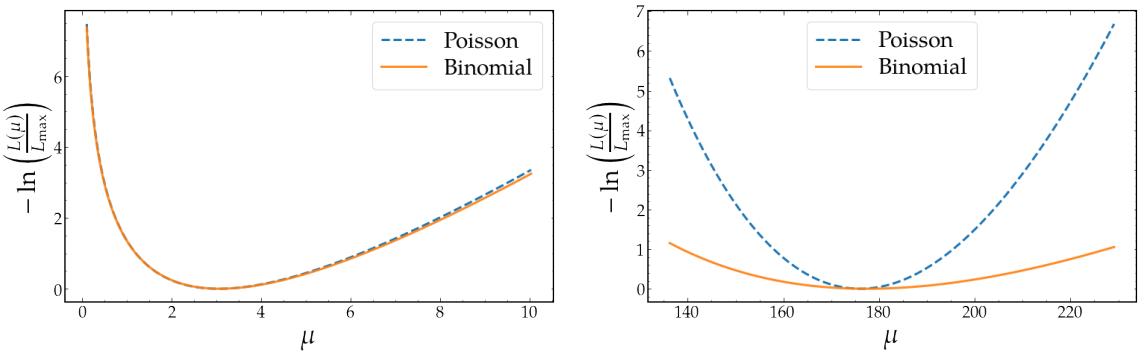

Figure 1: Poisson and binomial log-likelihoods for $k = 3$ (left) and $k = 60$ (right).

probability, $p_{\rm cc}(\theta, \phi)$, a data-driven quantity. The procedure for estimating this parameter is described in a separate contribution to these proceedings (see Ref. [8]). Therefore, the current estimator for the number of muons now reads

$$\hat{N}_\mu = -\frac{64}{1 + p_{\rm cc}(\theta, \phi)} \ln(1 - k/64). \tag{2}$$

Lastly, the single detector likelihood of Eq. (1) was replaced. Although the true number of muons in a detector does follow a Poisson distribution, the estimator $\hat{N}_\mu$ has additional fluctuations arising from the reconstruction procedure. Thus, Eq. (1) is sub-optimal as it underestimates the fluctuations of the detector signal. In Ref. [9], an improved likelihood model was developed, accounting for additional fluctuations arising from the segmentation of the UMD, which deviates from an ideal Poissonian counter. The exact distribution of the number of triggered bars k in a detector was derived for a fixed μ, given by a binomial distribution with $n = 64$ trials and probability $p = 1 - e^{-\mu(\vec{p})}$. In order to account for corner-clipping muons, we replace μ with $\mu(1 + p_{\rm cc})$, as explained in Ref. [8]. The current likelihood thus reads as

$$L_{\rm binomial}(\vec{p}) = \binom{64}{k} e^{-\mu(1+p_{\rm cc}(\theta,\Delta\phi))} (e^{\mu(1+p_{\rm cc}(\theta,\Delta\phi)/64} - 1)^k. \tag{3}$$

In Fig. 1, the Poisson and binomial log-likelihoods are displayed as a function of μ for a detector with $k = 3$ (left panel) and $k = 60$ (right panel). When the multiplicity is low (e.g., $k = 3$), Poissonian fluctuations in the number of muons dominate, and the two curves show little difference. In contrast, for large signals (e.g., $k = 60$), Poisson fluctuations are reduced, and detector segmentation becomes dominant. Assuming a Poisson likelihood, in this case, underestimates the fluctuations (the Poisson curve is narrower than the binomial), leading to an overestimation of the weight of detectors with large signals in the LDF.

Analogous to the previous procedure, the event log-likelihood is constructed using the detector likelihoods from Eq. (3) and minimized to determine the optimal LDF parameters.

3.3 Performance of the different likelihoods

As previously said, a detailed discussion on time windows in the reconstruction can be found in Ref. [7], while the new data-driven corner-clipping correction is assessed in Ref. [8]. This work

focuses on the impact of transitioning from the Poisson paradigm of Eq. (1) to the binomial one of Eq. (3). A first comparison of these methods using a simplified toy Monte Carlo was presented in Ref. [9], which excluded detailed simulations of particle tracking, SD response, UMD electronics, corner-clipping muons, and detector inefficiencies. Here, we evaluate the two likelihoods using full detector simulations based on a library of CORSIKA [10] showers (proton and iron primary species) at energies of $10^{17.5}$, 10^{18}, and $10^{18.5}$ eV and zenith angles of 0, 12, 22, 32, 38, and 48 degrees. EPOS-LHC [11, 12] was employed as the hadronic interaction model. Particle propagation through the soil, the simulation of the detector electronics, and event reconstruction were performed using Offline , the Observatory's official software framework [13].

For each event, the true muon density at 450 m (ρ_{450}) — our muonic shower size — was compared to the reconstructed estimate ($\hat{\rho}_{450}$) to assess the bias in the LDF fit. The reconstruction was performed using both likelihoods: the Poisson method, which estimates muons via Eq. (2) and introduce it in Eq. (1), and the binomial method, which directly uses the detector signal k in Eq. (3). We employed a modified Nishimura-Kamata-Greisen (NKG) function as our LDF model:

$$\rho(r) = \rho_{450} \left(\frac{r}{450\ \mathrm{m}}\right)^{-\alpha} \left(\frac{1 + r/r_0}{1 + 450\ \mathrm{m}/r_0}\right)^{-\beta} \left(\frac{1 + (r/10r_0)^2}{1 + (450\ \mathrm{m}/10r_0)^2}\right)^{-\gamma}, \tag{4}$$

where $\alpha = 0.75$, $\gamma = 3$ and $r_0 = 320$ m are fixed. The parameter β governs the slope of the LDF around the reference distance of 450 m. In some measured air-shower events, especially for lower energies, the low number of triggered stations and/or their positions around 450 m prevent them from leaving β free during the fit. Thus, β has to be fixed to a parameterized value obtained with a subset of events that fulfill a lever-arm criterium, consisting of having enough detectors with appropriate spacing around 450 m.

To perform an analysis similar to that in data, we first proceed to parameterize β and investigate the potential impact of the different likelihoods in this parameter. In Fig. 2, the mean β as a function of $\sec\theta$ is displayed for proton (left panel) and iron (right panel) and for the three energies in the library. The results show only a minor difference at $10^{18.5}$ eV (1-3%) between the β retrieved by the likelihoods, which is negligible for all practical purposes. We thus conclude that both likelihoods lead to compatible parameterizations of β.

The evolution of β was fitted with a linear model $\langle\beta\rangle = m(\sec\theta - 1.2) + b$ for each energy and primary (dashed lines in Fig. 2). Combining the results of both primaries and energies, a global parameterization, with an energy-independent slope m and an offset b linearly dependent on log-energy, was obtained. This parameterization was used to fix β in all the simulated events.

In Fig. 3, the bias and resolution of $\hat{\rho}_{450}$ are displayed as a function of energy for each primary species and likelihood model. No dependence on the zenith angle was found. The two likelihoods yield compatible biases and resolutions.

During the LDF fit, a 1σ error interval is computed for $\hat{\rho}_{450}$. In Fig. 4, the coverage of this interval for the Poisson (circles) and binomial (squares) likelihoods, calculated as the fraction of events where the interval includes the true ρ_{450}, is shown. The coverage of the Poisson likelihood decreases with energy, while the binomial likelihood remains stable around 60%. This difference arises because the Poisson model ignores detector segmentation, underestimating signal fluctuations — as already explained — and, thereby, the uncertainty interval. In contrast, the binomial model

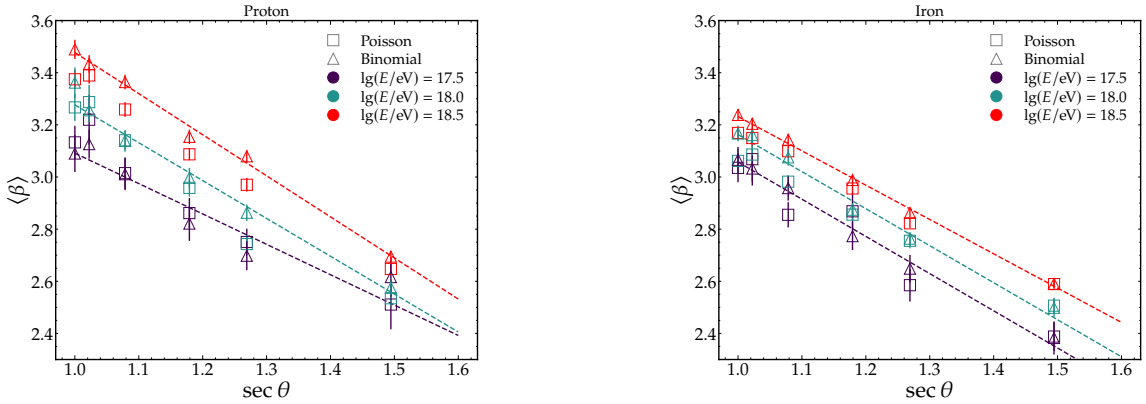

Figure 2: Mean β as a function of $\sec\theta$ for different energies using the Poisson (squares) and binomial (triangles) likelihoods. Left (right) panel shows proton (iron) simulations. The dashed lines indicate the results of the fits of the linear model.

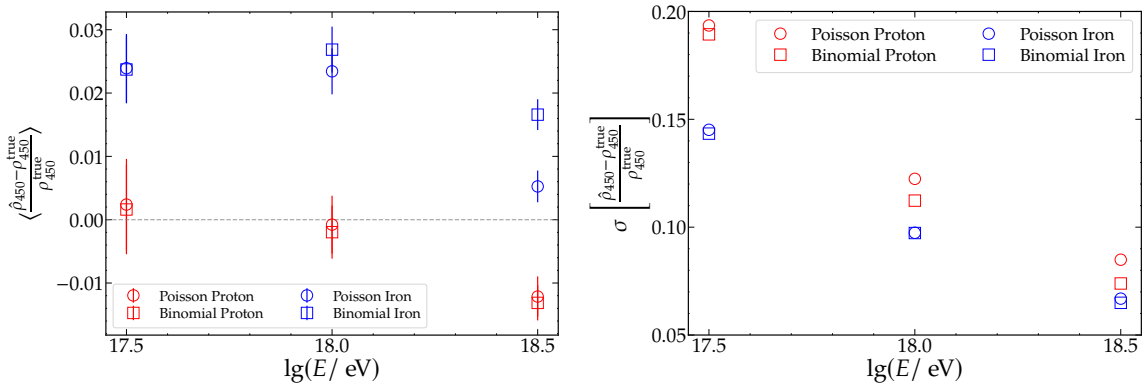

Figure 3: Bias (left) and resolution (right) as a function of Monte Carlo energy for the binomial and Poisson likelihoods.

accounts for segmentation, resulting in larger, more accurate uncertainty intervals and improved coverage.

4. Improved calibration of the ADC mode

As explained in Section 2, the mean charge deposited by a single vertical muon, $q_{1\mu}$, serves as the foundation for the reconstruction in the ADC mode. Determining this value is the goal of the calibration procedure.

The number of muons in a module is estimated using

$$\hat{N}\mu^{\mathrm{ADC}} = \frac{q\cos\theta}{q_{1\mu}}, \tag{5}$$

where q represents the charge of the ADC signal. Since the charge increases as $\sec\theta$ due to the increased muon track length in the detector, multiplying by $\cos\theta$ is necessary to cancel this effect.

The parameter $q_{1\mu}$ must also account for the charge deposited by accompanying knock-on electrons produced as the muon traverses the soil. These electrons are more likely to be produced

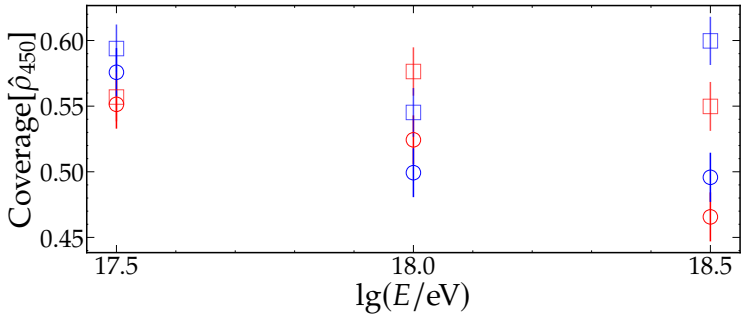

Figure 4: Coverage of the 1σ interval of $\hat{\rho}_{450}$ as a function of Monte Carlo energy for the binomial (squares) and Poisson (circles) likelihoods. Blue (red) markers correspond to iron (proton) primaries.

and with higher energy as the kinetic energy of the muon increases. Since higher-energy muons are generated closer to the shower core, $q_{1\mu}$ increases closer to the core due to the contribution of knock-on electrons. This dependence on the distance needs to be accounted for in Eq. (5) to produce an unbiased estimate. A detailed study on the contribution of non-muonic particles to the detector signal can be found in a separate contribution to these proceedings [14].

The following formula is used to estimate $q_{1\mu}$

$$q_{1\mu} = \frac{q \cos\theta}{\hat{N}_{\mu}^{\text{bin}}}, \tag{6}$$

where $\hat{N}_{\mu}^{\text{bin}}$ corresponds to the estimated number of muons with the binary mode with Eq. (2). In the left panel of Fig. 5, $q_{1\mu}$ as a function of the distance for a 10 m^2 module using simulations is displayed. Due to the aforementioned effect of the knock-on electrons, $q_{1\mu}$ increases closer to the core. Thus, $q_{1\mu}$ is parameterized with the model

$$q_{1\mu} = A \log_{10}(r/m) + B, \tag{7}$$

where A and B are fit parameters. In the right panel of the figure, the bias of Eq. (5) is shown as a function of the true number of injected muons for two cases: one where the dependence of $q_{1\mu}$ on r is accounted for (solid markers) and one where it is not (empty markers). In the latter case, $q_{1\mu}$ is obtained as the mean charge recorded when single vertical muons are injected into the detector, following the energy distribution of atmospheric muons. With this procedure, the bias increases with the number of muons. Since modules with a large number of muons are produced closer to the core, they are more affected by knock-on electrons. Conversely, when the distance dependence is taken into account via Eq. (7), the bias remains flat and below 2%.

5. Summary

The current status of the UMD reconstruction procedure has been presented. In the binary mode, the use of time windows has been discarded, and a new data-driven corner-clipping correction has been included. Additionally, the likelihood model for LDF fitting was switched from Poisson to binomial. This work focused on the impact of this change, showing that the two methods yield

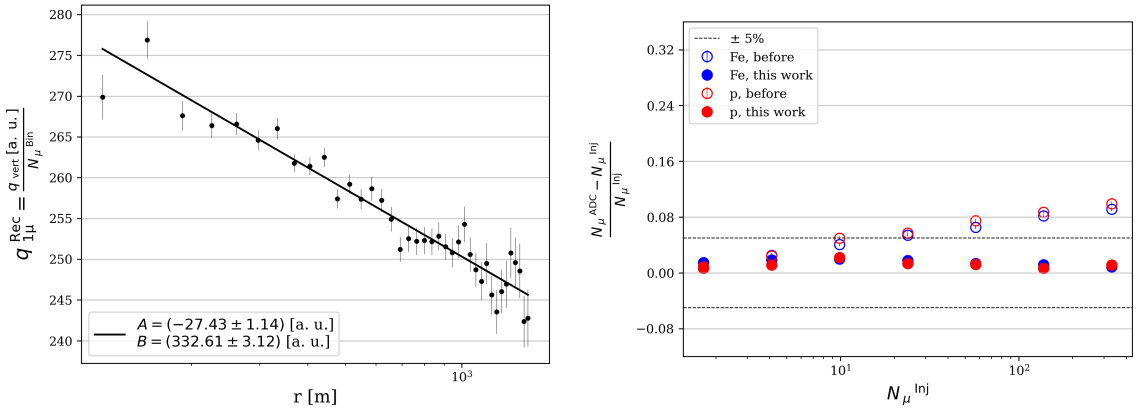

Figure 5: *Left*: Single muon charge obtained with Eq. (6) as a function of the distance to the shower axis. The solid line indicates the fit to the model of Eq. (7). *Right*: Bias of Eq. (5) as a function of the true number of muons.

compatible biases and resolution for the muonic shower size. However, the binomial likelihood provides broader coverage due to improved error estimation.

An improved method for determining the mean charge of a single vertical muon, the key parameter for reconstruction in ADC mode, has been introduced. This method accounts for the dependence of the parameter on the distance to the core, incorporating the contribution of knock-on electrons. The new method achieves a bias below 2%. Ongoing work includes applying this method to data, which will enable the use of ADC measurements where the binary mode saturates, enhancing the LDF reconstruction.

References

[1] The Pierre Auger Collaboration, JINST **15** (2020) P10021
[2] The Pierre Auger Collaboration, Nucl. Instrum. Meth. A **620** (2010) 227-251
[3] A. Castellina for the Pierre Auger Collaboration, EPJ Web Conf. **210** (2019) 06002.
[4] The Pierre Auger Collaboration, JINST **16** (2021) P04003.
[5] A. D. Supanitsky *et al.*, Astropart. Phys. **29** (2008) 461-470.
[6] The Pierre Auger Collaboration, Eur. Phys. J. C **80** (2020) 1-19.
[7] F. Gesualdi and A. D. Supanitsky, Eur. Phys. J. C **82** (2022) P925.
[8] J. de Jesús, J. M. Figueira, F. Sanchez, D. Veberič, *PoS* **UHECR2024** (2024) 078
[9] Ravignani, D. and Supanitsky, A. D., Astropart. Phys. **65** (2015) 1–10.
[10] D. Heck *et al.*, **Report FZKA** (1998) 6019
[11] K. Werner *et al.*, *Phys. Rev. C* **74** (2006) 044902.
[12] T. Pierog *et al.*, *Phy. Rev. C* **92** (2015) 034906.
[13] S. Argiro et al., Nucl. Instrum. Meth. A **580** (2007) 1485
[14] M. Scornavacche, J.M. Figueira, F. Sanchez and D. Veberič, *PoS* **UHECR2024** (2024) 116